Dalton Transactions

Accepted Manuscript

ROYAL SOCIETY OF CHEMISTRY

www.rsc.org/dalton

Graphical Abstract

Paramita Kar,Yumi Ida, Takuya Kanetomo, Michael G. B. Drew, Takayuki Ishida and Ashutosh Ghosh

---

A pyrazine bridged 1D coordination polymer of Mn(II) has been oxidized by *n*-Bu_4NMnO_4 to hexanuclear Mn(II/III) complexes. Their catecholase-like activities and magnetic interactions have been studied.

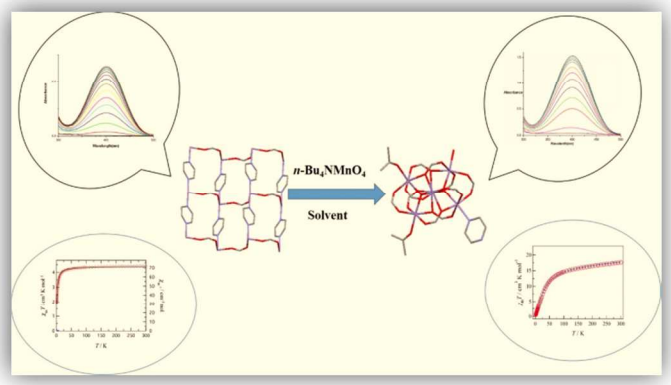

Cite this: DOI: 10.1039/c0xx00000x

www.rsc.org/xxxxxx

ARTICLE TYPE

Synthesis of mixed-valence hexanuclear Mn(II/III) clusters from its Mn(II) precursor: Variations of catecholase-like activity and magnetic coupling

Paramita Kar,[a] Yumi Ida,[b] Takuya Kanetomo,[b] Michael G. B. Drew,[c] Takayuki Ishida[b]* and Ashutosh Ghosh[a]*

Received (in XXX, XXX) Xth XXXXXXXXX 20XX, Accepted Xth XXXXXXXXX 20XX

DOI: 10.1039/b000000x

One Mn(II) coordination polymer, $[Mn(o\text{-}(NO_2)C_6H_4COO)_2(pyz)(H_2O)]_n$ (**1**) has been synthesized and oxidized by n-Bu_4NMnO_4 in non-aqueous media to two mixed-valence hexanuclear Mn(II/III) complexes $[Mn^{III}_2Mn^{II}_4O_2(pyz)_{0.61}/(MeOH)_{0.39}(o\text{-}(NO_2)C_6H_4COO)_{10}\cdot(H_2O)\cdot\{(CH_3)_2CO\}_2]\cdot(CH_3)_2CO$ (**2**) and $[Mn^{III}_2Mn^{II}_4O_2(pyz)_{0.28}/(MeCN)_{3.72}(o\text{-}(NO_2)C_6H_4COO)_{10}\cdot(H_2O)]$ (**3**) (where pyz = pyrazine). All three complexes were characterized by elemental analyses, IR spectroscopy, single-crystal X-ray diffraction analyses, and variable-temperature magnetic measurements. The structural analyses reveal that complex **1** is comprised of linear chains of pyz bridged Mn(II), which are further linked to one another by syn-anti carboxylate bridges, giving rise to a two-dimensional (2D) net. Complexes **2** and **3** feature mixed valence $[Mn^{III}_2Mn^{II}_4]$ units in which each of the six manganese centres reside in an octahedral environment. Apart from the variations in terminal ligands (acetone for **2** and acetonitrile for **3**), the complexes are very similar. Using 3,5-di-tert-butyl catechol (3,5-DTBC) as the substrate, the catecholase-like activity of the complexes has been studied and it is found that the mixed valent Mn_6 complexes (**2** and **3**) are much more active towards aerial oxidation of catechol compared to the Mn(II) complex (**1**). Variable-temperature (1.8-300 K) magnetic susceptibility measurements showed the presence of antiferromagnetic coupling in all three complexes. The magnetic data have been fitted with a 2D quadratic model derived by Lines, giving the exchange constant $J/k_B = -0.0788(5)$ K for **1**. For **2** and **3**, antiferromagnetic interactions within the Mn_6 cluster have been fitted with models containing three exchange constants: $J_A/k_B = -70$ K, $J_B/k_B = -0.5$ K, $J_C/k_B = -2.9$ K for **2** and $J_A/k_B = -60$ K, $J_B/k_B = -0.3$ K, $J_C/k_B = -2.8$ K for **3**.

Introduction

Among the transition metal ions, manganese-based coordination compounds have received considerable interest in the fields of supramolecular chemistry and crystal engineering not only for their remarkable magnetic properties,[1] but also for their rich biochemistry[2,3] and versatile catalytic activities.[4] The magnetic properties of such species are fascinating as the number and symmetry of the magnetic orbitals of the metal ion along with their possible overlap through the bridging ligand account for the ferro- or antiferromagnetic nature of the magnetic coupling.[5] In this regard, the hexanuclear mixed-valence carboxylate based clusters $[Mn_6O_2(RCO_2)_{10}L_4]$ deserve special mention for their magnetic properties at very low temperatures which have given rise to a specific family of single-molecule magnets (SMMs).[6] Several approaches leading to the isolation of hexanuclear manganese complexes with the $[Mn^{II}_4Mn^{III}_2O_2]^{10+}$ core are known.[7-10] The first one is based on $Mn^{II}(O_2CR)_2$ oxidation with oxygen,[7a] or MnO_4^-.[7b] The second involves reduction and subsequent coupling of trinuclear $[Mn^{II}Mn^{III}_2O]^{6+}$ species resulting in the formation of the $[Mn^{II}_4Mn^{III}_2O_2]^{10+}$ core.[8] The third method involves construction of the $[Mn^{II}_4Mn^{III}_2O_2]^{10+}$ unit by reduction of a species containing the $[Mn^{III}_4O_2]^{8+}$ core[9] and finally $[Mn^{II}_4Mn^{III}_2O_2]^{10+}$ species can be obtained by a reductive cleavage of complexes containing the $[Mn^{III}_8Mn^{IV}_4O^{12}]^{16+}$ core.[10]

The hexanuclear mixed-valence carboxylate based Mn_6 clusters possess the following common features: (i) the central core contains six manganese centres, two Mn(III) and four Mn(II) ions; (ii) the metal atoms are located in the vertex of two Mn^{II}_2-Mn^{III}_2 tetrahedra sharing their Mn(III)−Mn(III) edge with a μ_4 oxygen atom in the centre of each tetrahedron and there are four coordinated solvent molecules to four peripheral Mn(II) centres a distorted tetrahedral disposition. Recently, our group has replaced these solvent molecules by linear linker pyrazine to produce a mixed-valence Mn_6 unit based 3D diamondoid multifunctional (antiferromagnetism, gas adsorption and catechol oxidation) framework $[Mn^{III}_2Mn^{II}_4O_2(pyz)_2(C_6H_5CH_2COO)_{10}]_n$. The species was obtained by aerial oxidation of its Mn(II) precursor i.e. $[Mn^{II}(pyz)(C_6H_5CH_2COO)_2]$.[11] Our group has also reported a mixed-valence hexanuclear complex $[Mn^{III}_2Mn^{II}_4O_2(hmt)_4(OBz)_{10}]$ (hmt = hexamethylenetetramine and OBz = benzoate) which in acetonitrile medium spontaneously forms a self-assembled vesicular structure that encapsulated organic dye molecules, and also exhibits substantial catecholase-

like activity.[12] These results have inspired us to generate new Mn_6 based materials. To serve this purpose, we use here *o*-nitrobenzoate as carboxylate group. However, *o*-nitrobenzoate and pyz based Mn(II) precursors cannot be aerially oxidized to mixed-valence Mn_6 clusters unlike their phenylacetate analogues, rather, it requires an oxidizing agent e.g. MnO_4^-.

Herein, we report the crystal structures, magnetic properties and catecholase-like activities of one Mn(II) coordination polymer, $[Mn(o\text{-}(NO_2)C_6H_4COO)_2(pyz)(H_2O)]_n$ (**1**) and two mixed-valence hexanuclear Mn(II/III) complexes $[Mn^{III}_2Mn^{II}_4O_2(pyz)_{0.61}/(MeOH)_{0.39}(o\text{-}(NO_2)C_6H_4COO)_{10}\cdot(H_2O)\cdot\{(CH_3)_2CO\}_2]\cdot(CH_3)_2CO$ (**2**) and $[Mn^{III}_2Mn^{II}_4O_2(pyz)_{0.28}/(MeCN)_{3.72}(o\text{-}(NO_2)C_6H_4COO)_{10}\cdot(H_2O)]$ (**3**) (where pyz = pyrazine) which have been synthesized by oxidation of **1** by n-Bu_4NMnO_4 in non-aqueous medium i.e. methanol and then the oxidized products are recrystallized from acetone (for **2**) and acetonitrile (for **3**). In complex **1**, linear chains of pyz bridged Mn(II) are further linked to one another by *syn-anti* carboxylate bridges, giving rise to a two-dimensional (2D) net. Complexes **2** and **3** feature mixed valence $[Mn^{III}_2Mn^{II}_4]$ units. The catalytic activities and the antiferromagnetic exchange couplings of **2** and **3** are much higher than those of complex **1**. It is notable that although the synthesis and structure of $[Mn_6O_2(RCOO)_{10}]$ clusters are quite common,[13] we report here for the first time the generation of mixed-valent Mn_6 clusters by oxidizing the corresponding structurally characterized 1D coordination polymer (complex **1**) using n-Bu_4NMnO_4 as oxidant and the corresponding changes in the magnetic and catalytic properties.

Experimental Section

$Mn(o\text{-}(NO_2)C_6H_4COO)_2\bullet H_2O$ was synthesized by the procedure described previously.[14] All other chemicals purchased were of reagent grade and used without further purification.

Synthesis of $[Mn(o\text{-}(NO_2)C_6H_4COO)_2(pyz)(H_2O)]_n$ (1). A methanolic (10 mL) solution of pyz (0.160 g, 2 mmol) was added to a solution of $Mn(o\text{-}(NO_2)C_6H_4COO)_2\bullet H_2O$ (0.405 g, 1 mmol) in 5 mL of methanol. The resulting mixture was refluxed for about 2 h, cooled, and filtered. The resulting clear filtrate gave a pale yellow solid on standing for 1−2 days at room temperature. The yellow solid was re-dissolved in CH_3OH and filtered. Yellow colored plate-like single-crystals suitable for X-ray diffraction were obtained by slow evaporation of the mother liquor after several days.

Complex **1**: Yield: 0.361 g; 76%. Anal. Calcd. for $C_{18}H_{14}MnN_4O_9$ (485.27): C, 44.55; H, 2.91; N, 11.55 Found: C, 44.31; H, 2.97; N, 11.39. IR (KBr pellet, cm^{-1}): 1612, 1531 ν_{as}(COO), 1405, 1365 ν_s(COO).

Synthesis of $[Mn^{III}_2Mn^{II}_4O_2(pyz)_{0.61}/(MeOH)_{0.39}(o\text{-}(NO_2)C_6H_4COO)_{10}\cdot(H_2O)\cdot\{(CH_3)_2CO\}_2]\cdot(CH_3)_2CO$ (2) and $[Mn^{III}_2Mn^{II}_4O_2(pyz)_{0.28}/(MeCN)_{3.72}(o\text{-}(NO_2)C_6H_4COO)_{10}\cdot(H_2O)]$ (3). To a methanolic solution (20 mL) of complex **1** (2.43 g, 5 mmol) solid n-Bu_4NMnO_4 (0.57 g, 1.58 mmol) was added in small portions with constant stirring when the solution turned to deep brown. After half an hour, it was filtered. The resulting clear filtrate gave a brown solid on standing overnight at room temperature. The brown precipitate was collected by filtration and dissolved in acetone (30 mL) and brown colored plate-like single-crystals of complex **2** suitable for X-ray diffraction were obtained by slow evaporation of the filtrate after several days.

Complex **3** was obtained by following a procedure similar to that of **2**, the only difference being that the brown precipitate was re-dissolved in acetonitrile (30 mL).

Complex **2**: Yield: Yield: 0.271 g; 73%. Anal. Calcd. for $C_{80.98}H_{62.08}Mn_6N_{11.15}O_{46.17}$ (2259.87): C, 43.04; H, 2.77; N, 6.91 Found: C, 43.11; H, 2.91; N, 6.82. IR (KBr pellet, cm^{-1}): 1596 ν_{as}(COO), 1395 ν_s(COO).

Complex **3**: Yield: 0.242 g; 68%. Anal. Calcd. for $C_{78.45}H_{52.23}Mn_6N_{14.23}O_{42}$ (2195.84): C, 42.91; H, 2.40; N, 9.08 Found: C, 42.89; H, 2.47; N, 9.11. IR (KBr pellet, cm^{-1}): 1593 ν_{as}(COO), 1389 ν_s(COO).

Alternative Method for the Synthesis of Compounds 2 and 3.

To a methanolic solution (20 mL) of $Mn(o\text{-}(NO_2)C_6H_4COO)_2\bullet 3H_2O$ (2.025 g, 5 mmol) was added pyz (0.400 g, 5 mmol) to give a pale yellow solution. This was stirred while solid n-Bu_4NMnO_4 (0.57 g, 1.58 mmol) was added in small portions over approximately half an hour; the solution turned deep brown. Overnight storage gave a brown precipitate, which was collected by filtration and dissolved in acetone (30 mL) (for **2**) and in acetonitrile (30 ml) (for **3**). Brown coloured plate-like single crystals of complexes **2** and **3** suitable for X-ray diffraction were obtained by slow evaporation of the corresponding filtrates after several days.

Physical measurements

Elemental analyses (carbon, hydrogen, and nitrogen) were performed using a Perkin-Elmer 240C elemental analyzer. IR spectra in KBr (4500−500 cm^{-1}) were recorded using a Perkin-Elmer RXI FT-IR spectrophotometer. Electronic absorption spectra (1000−200 nm) were recorded in CH_3CN with a Hitachi U-3501 spectrophotometer. Magnetic susceptibilities on polycrystalline samples were measured on a QuantumDesign SQUID magnetometer (MPMS-7) at applied magnetic fields of 5000 Oe in a temperature range of 1.8–300 K. The magnetic response was corrected with diamagnetic blank data of the sample holder obtained separately. The diamagnetic contribution of the sample itself was estimated from Pascal's constant.

Crystal data collection and refinement

Suitable single crystals of each complexes were mounted on a Bruker SMART diffractometer equipped with a graphite monochromator and 3405, 16903, 16277 independent reflection data for **1**, **2** and **3** were collected with Mo-Kα (λ = 0.71073 Å) radiation at 293K. The crystals were positioned at 60 mm from the CCD. 360 frames were measured with a counting time of 10 s. The non-hydrogen atoms were refined with anisotropic thermal parameters. Hydrogen atoms were placed in idealized positions

and their displacement parameters were fixed to be 1.2 times larger than those of the attached non-hydrogen atom. Successful convergence was indicated by the maximum shift / error of 0.001 for the last cycle of the least squares refinement. Absorption corrections were carried out using the SADABS program.[15] Structures **2** and **3** showed disorder in the solvent molecules including those bound to the metal. In **3**, one of the nitro groups was disordered over two positions. In such cases, occupation factors were refined and distance constraints were used where necessary. All calculations were carried out using SHELXS 97,[16] SHELXL 97,[17] PLATON 99,[18] ORTEP-32[19] and WinGX systemVer-1.64.[20] The three structures were refined using Shelxl97[17] on F^2 to $R1$ 0.0690, 0.0574 0.0442; $wR2$ 0.1892, 0.1282, 0.1049 for 2842, 10549, 12275 data with $I>2\sigma(I)$. Data collection and structure refinement parameters and crystallographic data for the three complexes are given in Table 1.

Results and Discussion

Synthesis. The Mn(II) coordination polymer (complex **1**) has been synthesized as a light-yellow crystalline solid by self-assembly of the primary ligand i.e. the Mn(II) salt of o-nitrobenzoate together with pyz as the secondary spacer in methanol solution at ambient temperature in 1:1 molar ratios. For the preparation of complexes with the $[Mn^{II}_4Mn^{III}_2O_2]^{10+}$ core by aerial oxidation, acetonitrile is the most commonly used solvent,[8a,21] Previously, we reported a mixed-valence hexanuclear Mn(II/III) cluster which was obtained by aerial oxidation of Mn(II) precursor.[11] Following the similar procedure here also, we dissolved complex **1** in CH_3CN, but after one week, a yellow crystalline solid reappeared indicating that aerial oxidation of the complex did not take place in this medium. We changed solvents from acetonitrile to dichloromethane, acetone and ethanol but in no case did aereal oxidation occur. By comparison of these results with those of Mn(II) benzoate, it is obvious that introduction of the $-NO_2$ group to the phenyl ring prevents the aerial oxidation of the Mn(II) complex. Therefore, n-Bu_4NMnO_4, a reagent well known for oxidation of Mn(II) species to mixed-valence entity in non-aqueous solvents, was used. To crystallize the brown colored oxidized amorphous solid obtained from methanol, it was dissolved in acetonitrile, dichloromethane, acetone and ethanol and obtained single crystals of complexes **2** and **3** from acetone and acetonitrile, respectively.

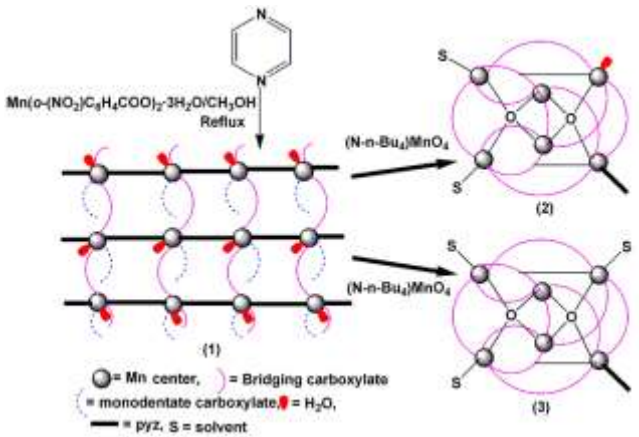

Scheme 1: Formation of complexes.

Table 1 Crystal data and structure refinement parameters for complexes **1-3**.

	1	**2**	**3**
Formula	$C_{18}H_{14}MnN_4O_9$	$C_{80.98}H_{62.08}Mn_6N_{11.15}O_{46.17}$	$C_{78.45}H_{52.23}Mn_6N_{14.23}O_{42}$
Formula weight	485.27	2259.87	2195.84
Space group	$Pn2_1a$	$Pbca$	$P2_1/n$
Crystal system	Orthorhombic	Orthorhombic	Monoclinic
a/ Å	8.889(5)	22.618(5)	13.408(5)
b/ Å	7.407(5)	27.352(5)	27.548(5)
c/ Å	30.467(5)	30.830(5)	24.733(5)
β/deg	90	90	99.406(5)°
V/Å^3	2006.0(18)	19073(6)	9013(4)
Z	4	8	4
Calculated density D_{calc}/g cm^{-3}	1.607	1.575	1.618
Absorption coeff.(μ) mm^{-1}	(MoKα) 0.719	(MoKα) 0.873	(MoKα) 0.919
F(000)	988	9169	4434
R(int)	0.059	0.067	0.036
θ range (deg)	1.34 to 25.06	1.32 to 25.34	1.1 to 25.4
Total reflections	8664	86170	62179
Unique reflections	3405	16903	16277
Observed data $I>2\sigma(I)$	2842	10549	12275
$R1$, $wR2$	0.0690, 0.1892	0.0574, 0.1555	0.0442, 0.1178

Journal Name

Cite this: DOI: 10.1039/c0xx00000x

www.rsc.org/xxxxxx

ARTICLE TYPE

Description of structures

The structure of **1** is shown in Figure 1 together with the atomic numbering scheme in the metal coordination sphere.

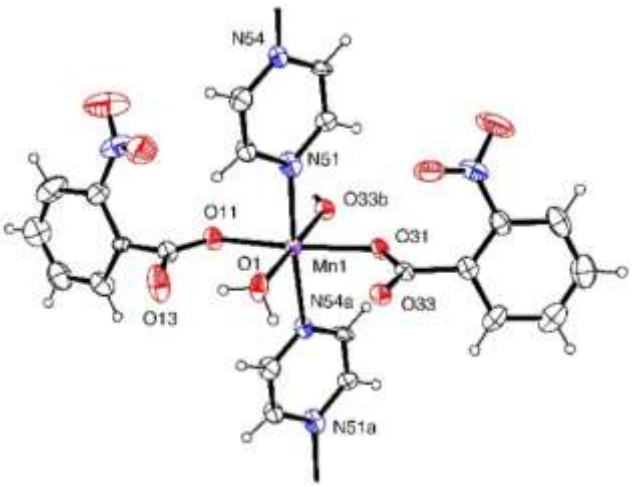

Fig. 1 The coordination environments of the Mn(II) ion in complex **1** (symmetry codes a = *x*,1+*y*,*z*, b = -1/2+*x*, *y*, 1/2-*z*) with ellipsoids at 30% probability

The manganese atom occupies a distorted octahedral environment. In the equatorial plane it is bonded to two monodentate (*o*-$(NO_2)C_6H_4COO$) groups through O(11) and O(31) at 2.122(4) and 2.171(4) Å and to two pyz ligands through nitrogen atoms N(51) and N(54) (*x*,1+*y*,*z*) at 2.293(10) and 2.325(9) Å respectively. The axial positions are occupied by one water molecule O(1) at 2.153(5) Å and a bridging oxygen atom O(33) (-1/2+*x*, *y*, 1/2-*z*) at 2.152(4) Å from (*o*-$(NO_2)C_6H_4COO$) (Table 2).

Table 2: Bond distances (Å) and angles (º) in the metal coordination sphere of complex **1:**

Atom labels	**Distance**	**Atom labels**	**Distance**
Mn(1)-O(11)	2.122(4)	Mn(1)-N(51)	2.293(10)
Mn(1)-O(1)	2.153(5)	Mn(1)-N(54)[a]	2.325(9)
Mn(1)-O(31)	2.171(4)	Mn(1)-O(33)[b]	2.152(4)
Atom labels	**Angles**	**Atom labels**	**Angles**
O(11)-Mn(1)-O(33)[b]	93.62(16)	O(11)-Mn(1)-O(1)	85.51(16)
O(33)[b]-Mn(1)-O(1)	179.0(3)	O(11)-Mn(1)-O(31)	174.27(18)
O(33)[b]-Mn(1)-O(31)	80.96(14)	O(1)-Mn(1)-O(31)	99.93(15)
O(11)-Mn(1)-N(51)	91.6(3)	O(33)[b]-Mn(1)-N(51)	91.6(3)
O(1)-Mn(1)-N(51)	89.0(3)	O(31)-Mn(1)-N(51)	86.7(3)
O(11)-Mn(1)-N(54)[a]	93.1(3)	O(33)[b]-Mn(1)-N(54)[a]	88.7(3)
O(1)-Mn(1)-N(54)[a]	90.8(3)	O(31)-Mn(1)-N(54)[a]	88.7(3)
N(51)-Mn(1)-N(54)[a]	175.3(2)		

Symmetry code: [a] = *x*, 1+*y*, *z*; [b] = -1/2+*x*, *y*, 1/2-*z*

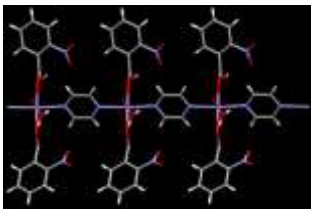

(a)

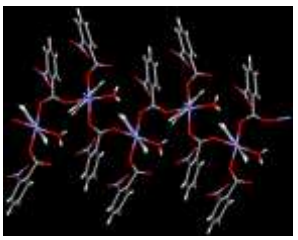

(b)

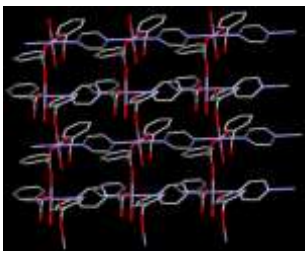

(c)

Fig. 2 Packing in **1**, (a) Formation of linear chain by pyrazine linkers; (b) Formation of linear chain by carboxylate oxygens; (c) Formation of two-dimensional framework.

The pyz ligands form a linear chain in the b direction via M-pyz-M-pyz-M links while the carboxylate oxygen O(33)[b] forms a Mn-O-Mn-O-Mn link in the a direction via glide plane. The structure is therefore a two-dimensional polymer.

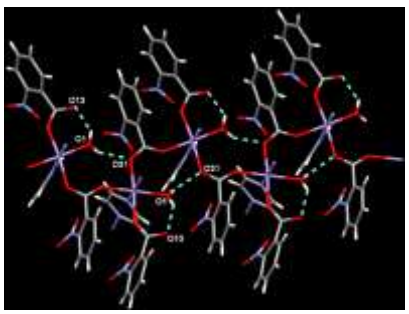

Fig. 3 Hydrogen-bonding interactions in compound **1** shown as dotted lines.

The water molecule O(1) forms two donor hydrogen bonds to O(13) and O(31) (-1/2+*x*, *y*, 1/2-*z*) with dimensions H...O 1.83, 2.38Å, O-H...O 2.621(7), 2.843(6) Å and O-H...O 153, 115° respectively

Both **2** and **3** contain discrete hexanuclear units. The complexes are completed by four terminal ligands; for **2**, these are two acetones, one water molecule together with one site disordered between ligand pyz at 61(1)% and acetone at 39(1)% occupancy. For **3** there are four acetonitriles of which one is disordered with 72(1)% occupancy together with a ligand pyz at 28(1) % occupancy.

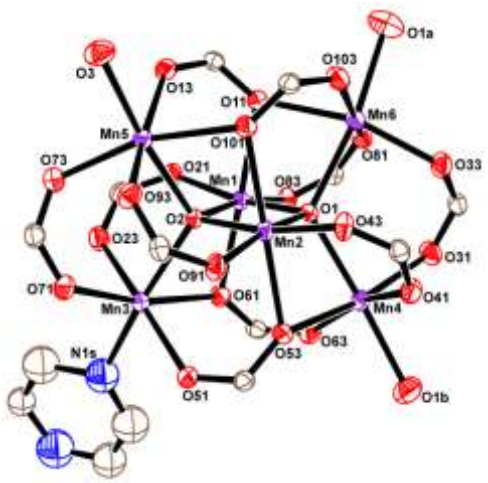

(a)

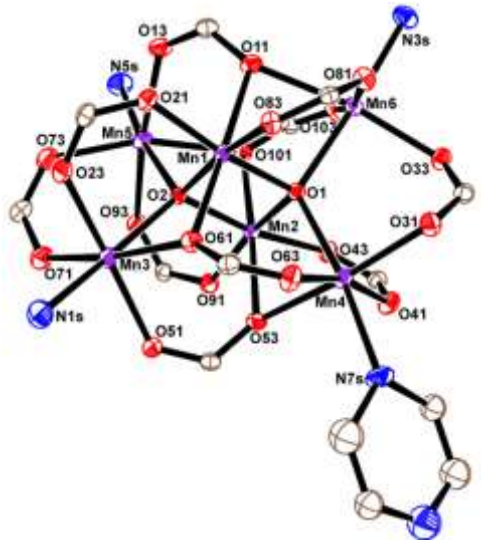

(b)

Fig. 4 Central [Mn_6] cluster in complexes **2** (a) and **3** (b) with ellipsoids at 30% probability. All hydrogen atoms and ortho-nitro benzoate rings have been omitted for clarity. For disordered terminal ligands, only the major component is shown. **2** contains disordered solvent molecules which are not shown.

Apart from these variations in terminal ligands, the complexes are very similar as is apparent from figures of **2** and **3** (Figure 4), and also when the dimensions of the structures, which are numbered equivalently, are compared in Table ST1 (supporting information). Indeed there are very few differences in the geometry of the $Mn_6(o\text{-}(NO_2)C_6H_4COO)_{10}$ moieties. In both structures, all six metal atoms occupy six-coordinate distorted octahedral environments. At the centre of Mn_6 core of both complexes there are two Mn(III) atoms, namely Mn(1) and Mn(2) which form the shortest contacts at 2.810(1) Å in **2** and 2.804(1) Å in **3**. The remaining four metal atoms in both structures are Mn(II). In **2**, Mn(1) is close to Mn(3) and Mn(6) at 3.1878(1) and 3.184(1) Å while Mn(2) is close to Mn(4) and Mn(5) at 3.180(1), 3.182(1) Å. Mn···Mn distances in **3** are comparable at 3.198(1), 3.183(1), 3.178(1), 3.190(1) Å respectively. Mn(1) and Mn(2) are bridged by O(1) and O(2) which each bridge two further Mn atoms, Mn(4), Mn(6) in the case of O(1) and Mn(3), Mn(5) in the case of O(2). In the two structures, the distances from the bridging oxygen atoms O(1) and O(2) to Mn(1) and Mn(2) are in the range 1.877(3)-1.899(2) Å while distances to the other metal atoms are in the range 2.196(2)-2.242(3) Å.

In addition to these bridging oxygen atoms Mn(1) and Mn(2) are each bonded to four oxygen atoms from four different *o*-nitro benzoates. Of these, two bonds, which are *trans* to the bridging oxygen atoms are shorter in the range 1.946(2)-1.978(3) Å and the other two which are mutually trans are longer in the range 2.204(3)-2.246(3) Å.

The four remaining metal atoms are also bonded to four oxygen atoms from four *o*-nitro benzoates, but also to one of the bridging oxygen atoms, either O(1) or O(2), and a terminal solvent ligand and these two atoms are mutually trans. Thus in the complexes all 20 oxygen atoms of the 10 *o*-nitro benzoates bridge with at least two different metal atoms but four namely O(11), O(53), O(61), O(101) are bonded to three metal atoms. As a consequence the Mn-O bonds containing these four atoms are among the longest.

The coordination spheres of these four metal atoms are completed by monodentate solvent ligands. In **2**, these are two $(CH_3)_2CO$ ligands and one water molecule while the fourth site is disordered between ligand pyz and methanol. By contrast in **3**, there are three acetonitrile molecules while the fourth site is disordered between a further acetonitrile and ligand pyz.

In **2**, there is an additional $(CH_3)_2CO$ solvent molecule, but **3** does not contain any unattached solvent. There are additional hydrogen bonds in **2**. In **2** the water molecule O(3) forms strong donor hydrogen bonds to the free solvent acetone molecule O(1C) (1-x, -y, -z) and to O(18) from a nitro group with dimensions 2.727(9), 1.87 Å, 174° and 2.992(7), 2.20 Å, 158° respectively.

Magnetic properties.

Figure 5 shows the temperature dependence of magnetic susceptibilities for **1** measured at an applied magnetic field of 5000 Oe. At 300 K, the $\chi_m T$ value was 4.42 cm^3 K mol^{-1}, which agrees well with S = 5/2 Mn^{II} ion and g = 2. The $\chi_m T$ value

monotonically decreased on cooling and reached 1.95 cm^3 K mol^{-1} at 1.8 K. This behavior indicates that antiferromagnetic coupling are dominant. As an empirical approach, the Curie-Weiss parameters have been determined as shown in Table 3.

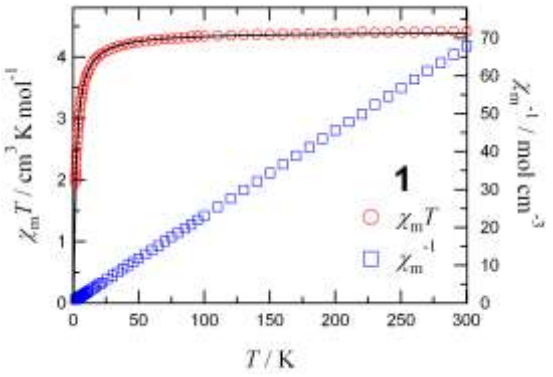

Fig. 5. Temperature dependences of the product of the magnetic susceptibility and temperature (right) and reciprocal magnetic susceptibility (left) for **1**, measured at 5000 Oe. The susceptibility was reduced to the mononuclear formula basis. Solid line shows the simulation curve from a 2D model (see the text).

Table 3. Curie-Weiss constants of **1**, **2** and **3**.

Curie-Weiss constants	**1**	**2**	**3**
C/cm^3 K mol^{-1}	4.449(2)	20.02(3)	20.99(5)
θ/K	–2.50(9)	–33.4(7)	–38.0(10)
Temp. range for Curie-Weiss fitting	50-300 K	50-300 K	50-300 K
χT/cm^3 K mol^{-1}	4.42 (300 K)	18.2 (300 K)	18.9 (300 K)
H (Oe)	5000	5000	5000
G	2.00	1.97	2.00

To evaluate the exchange coupling, we need to identify the dominant interaction pathways, in the metal organic framework of complex **1**. In the crystal lattice, the Mn(II) ions are doubly bridged with three atoms of the carboxylate groups, and this motif is repeated infinitely to give a 1D zigzag chain. The most important exchange coupling can be assigned to intrachain Mn···Mn interactions with equal spacing. The chains are connected with pyz, which may afford only auxiliary interactions because of the long distance (across four atoms). Therefore, the main exchange channel is assumed to be 1D. From the Fisher model[22] with $\hat{H} = -2J\Sigma S_i \cdot S_{i+1}$ we obtain $J/k_B = -0.143(1)$ K and $g = 2.005(2)$. Assuming that the exchange coupling occurs in a 2D quadratic manner, the Lines equation[23] can be used which gives $J/k_B = -0.0788(5)$ K and $g = 2.008(1)$. We need to consider a possible zero-field splitting effect, which leads to a decrease of the $\chi_m T$ product at low temperatures and therefore the J values obtained here may be overestimated

For the three atoms ($\mu_{1,3}$) carboxylate bridges, a *syn-anti* bridging configuration is rare by comparison with a *syn-syn* configuration.[24] It is expected on the basis of the respective geometries that an efficient overlap between the 3d magnetic orbital of the Mn^{2+} center and the 2p orbital of the carboxyl oxygen atom would lead to antiferromagnetic interaction through the $\mu_{1,3}$-carboxylate bridging ligand and depends on the coordination mode of the carboxylate ligand. *Syn-anti* carboxylato bridges induce smaller J values because of the expanded metallic core and a mismatch in the orientation of magnetic orbitals[24,25] which is in good agreement with the experimental observations.

Figure 6 shows the temperature dependence of magnetic susceptibilities for **2** and **3** measured at an applied magnetic field of 5000 Oe. At 300 K, the $\chi_m T$ values were 18.2 and 18.9 cm^3 K mol^{-1} for **2** and **3**, respectively, which are far below the theoretical spin-only values at high temperature limit (23.5 cm^3 K mol^{-1} from two $S = 2$ Mn^{III} ions and four $S = 5/2$ Mn^{II} ions with $g = 2$). The $\chi_m T$ values monotonically decreased on cooling and reached 0.525 and 1.18 cm^3 K mol^{-1} for **2** and **3**, respectively, at 1.8 K. No meaningful dynamic properties were found for **2** or **3** at 2 K. These findings indicate that antiferromagnetic couplings are dominant. As an empirical approach, the Curie-Weiss parameters have been determined as shown in Table 3. From the crystallographic analysis, the interaction can be reasonably attributed to the intramolecular exchange coupling in the Mn_6 cluster.

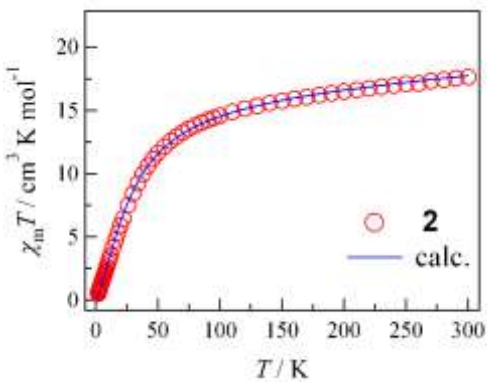

(a)

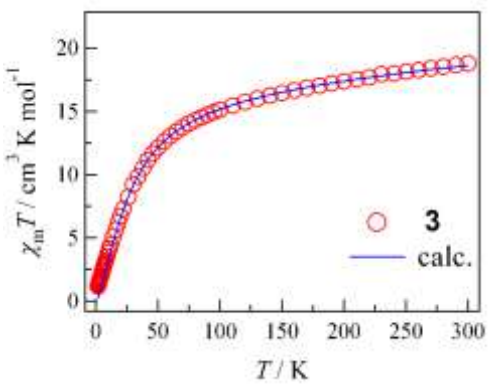

(b)

Fig. 6. Temperature dependence of the products of the magnetic susceptibility and temperature for **2** (a) and **3** (b), measured at 5000 Oe. Solid lines show the simulation (see the text).

To further investigate the magnetic coupling within a Mn_6 cluster, we define a spin exchange Hamiltonian for this system, so that the exchange parameters can be evaluated by simulation.

The exchange couplings among the Mn ions are classified as follows:

(1) Doubly μ_4-O bridged Mn^{III}---Mn^{III} (the exchange parameter is defined by J_A),

(2) Doubly μ_2-O and μ_4-O bridged Mn^{III}---Mn^{II} (by J_{B1}),

(3) Singly μ_4-O bridged Mn^{III}---Mn^{II} (by J_{B2}), and

(4) Singly μ_2-O bridged Mn^{II}---Mn^{II} (by J_C).

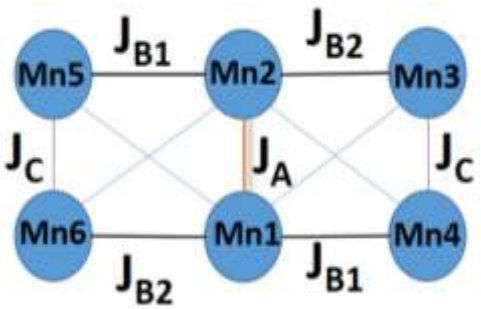

Fig. 7 Scheme of the magnetic exchange pathways in the $[Mn_6]$ cluster.

There are approximately four different magnetic interactions involved, corresponding to the Mn^{III}-Mn^{III}, Mn^{III}-Mn^{II} and Mn^{II}-Mn^{II} pathways. The Mn^{III}---Mn^{III} distances are very short, which may afford the strongest antiferromagnetic exchange coupling in such Mn_6 magnetic clusters. A close inspection at the Mn−O bond lengths in the oxido bridges shows that the double oxido bridge (O(1) and O(2)) connecting the two central Mn(III) ions (Mn(1) and Mn(2)) presents much shorter Mn−O bond lengths (Mn(1)−O(1) = 1.878(3) (for **2**) and 1.888(2) (for **3**) Mn(2)−O(1) = 1.900(3) Å) compared with the other Mn−O bond lengths.

To reduce the number of parameters, an approximation of $J_{B1} = J_{B2}$ was introduced, because their characteristics are similar with respect to the interacting species (Mn^{III} and Mn^{II}) and bridging motifs (Fig. 7). Therefore, the magnetic coupling parameters are defined as J_A, J_B and J_C, from the following Heisenberg spin Hamiltonian.[7a] Eq. (1) is utilized for **2** and **3**.

$$\hat{H} = -2J_A(\hat{S}_{Mn1}\cdot\hat{S}_{Mn2}) - 2J_B(\hat{S}_{Mn1}\cdot\hat{S}_{Mn3} + \hat{S}_{Mn1}\cdot\hat{S}_{Mn4} + \hat{S}_{Mn1}\cdot\hat{S}_{Mn5} + \hat{S}_{Mn1}\cdot\hat{S}_{Mn6} + \hat{S}_{Mn2}\cdot\hat{S}_{Mn3} + \hat{S}_{Mn2}\cdot\hat{S}_{Mn4} + \hat{S}_{Mn2}\cdot\hat{S}_{Mn5} + \hat{S}_{Mn2}\cdot\hat{S}_{Mn6}) - 2J_C(\hat{S}_{Mn3}\cdot\hat{S}_{Mn5} + \hat{S}_{Mn4}\cdot\hat{S}_{Mn6}) - -(1)$$

The parameters were optimized by simulation performed using the MAGPACK software.[26] The resultant curves are superimposed in Figure 6, and the experimental values were well reproduced. The best fit parameters were: $J_A/k_B = -70$ K, $J_B/k_B = -0.5$ K, $J_C/k_B = -2.9$ K, and $g = 1.97$ for **2** and $J_A/k_B = -60$ K, $J_B/k_B = -0.3$ K, $J_C/k_B = -2.8$ K, and $g = 2.00$ for **3**. Possible errors in the calculation of J parameters are estimated to be below 5%. The present parameters are reasonable for such Mn_6 clusters, as highly related $[Mn_6]$ systems were reported to show comparable values: e.g. $J_A/k_B = -60$ K, $J_B/k_B = -1.2$ K, and $J_C/k_B = -3.5$ K in $[Mn_6O_2(O_2CPh)_{10}(py)_2(MeCN)_2]$•2MeCN for example.[7a]

Even though the structure of the $[Mn_6O_2(RCOO)_{10}]$ cluster is quite common, only 18 of the 32 known examples have been magnetically characterized.[11,21,27a-g] All of them show moderate antiferromagnetic exchange couplings. The present study has shown that the most important feature responsible forthe magnetic properties is the presence of a strong magnetic coupling between the central Mn(III) ions, the other exchange pathways being less relevant. This strong coupling between the central Mn(III) ions correlates well with the expected value from magneto-structural correlations.

Catecholase-like Activity Study and Kinetics. Catechol oxidase catalyzes exclusively the oxidation of catechols (i.e., *o*-diphenols) to the corresponding quinones, and because of this oxidation process, known as catecholase activity (Scheme 2), catechol oxidase is able to play a key role for disease resistance in higher plants.

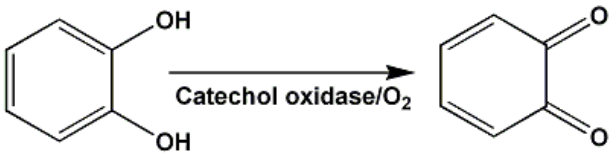

Scheme 2. Catecholase activity

Quinones are highly reactive compounds which undergo auto polymerization to produce melanin, a brown colored pigment, and this process is most likely responsible for protecting damaged tissues against pathogens and insects.

In most of the catecholase activity studies of model complexes, 3,5-di-*tert*-butylcatechol (3,5-DTBC) has been chosen as the substrate. Its low redox potential makes it easy to oxidize, and the bulky substituents prevent further reactions such as ring-opening.[28] The oxidation product 3,5-di-*tert*-butylquinone (3,5-DTBQ) is very stable and exhibits a maximum absorption at 403 nm in pure acetonitrile. The catecholase activity of complexes **1**–**3** was studied using 3,5-DTBC as a convenient model substrate, in air saturated acetonitrile solvent at room temperature (25 °C). For this purpose, solutions of the complexes were treated with 100 equiv. of 3,5-DTBC and the course of the reaction was followed by recording the UV–vis spectra of the mixture at an interval of 5 min. After addition of substrate 3,5-DTBC to the solutions of the catalysts **1**–**3**, a gradual increase of the band corresponding to 3,5-DTBQ was observed at ~400 nm (Fig. 8(a) and (b) for complexes **1** and **2** respectively and Fig. S1 for complex **3**).

This observation can be rationalised as follows. The oxidation of 3,5-DTBC to 3,5-DTBQ catalyzed by the complex, proceeds via the formation of a catalyst-substrate (CS) adduct whose λ_{max} is close to that of the complex itself. After a few minutes, the adduct slowly converts to the quinone[29] as observed in Figure 8. A control experiment has been carried out using Mn(*o*-$(NO_2)C_6H_4COO)_2 \cdot H_2O$ instead of the present complexes under

analogous conditions to study the possible catalytic activity of a simple Mn(II) salt in the oxidation of 3,5-DTBC to 3,5-DTBQ. Within 1 h of reaction no appreciable amounts of 3,5-DTBQ were observed using UV−vis spectroscopy (supporting information, Fig. S2).

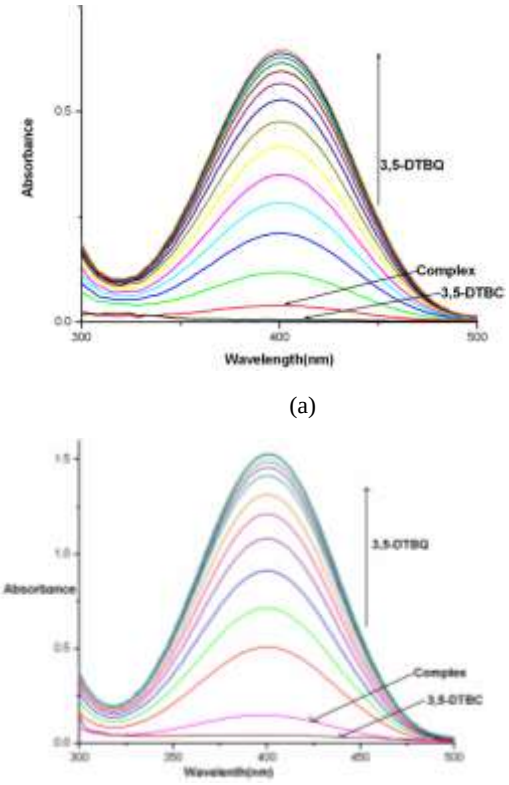

Fig. 8 Increase of absorption spectra after addition of 100 equiv of 3,5-DTBC to a solution containing complex **1** (1.00×10^{-4} M) (Fig. 8(a)) and complex **2** (0.166×10^{-5} M) (Fig. 8(b)) in acetonitrile. The spectra were recorded after every 5 min up to 1 h in CH_3CN.

Kinetic Study. The kinetic study of the oxidation of 3,5-DTBC to 3,5-DTBQ by complexes **1, 2** and **3** were carried out by monitoring the growth of the absorbance at ~400 nm by the initial rates method. To determine the dependence of the rates on the substrate concentration and various kinetic parameters, solutions of complexes **1** and **2** were prepared with increasing concentrations of 3,5-DTBC (from 10 to 100 equiv) under aerobic conditions at complex concentrations of 1.00×10^{-4} and 1.66×10^{-6} M respectively. Complex **3** exhibits almost similar behavior to that of complex **2**. A first-order dependence was observed at low concentrations of the substrate, whereas saturation kinetics was found at higher concentrations of the substrate, as shown in Figure 9 for complexes **1** and **2** (supporting information, Fig. S3 for complex **3**).

This dependence on the substrate concentration indicates that catalyst-substrate binding is the initial step in the catalytic mechanism. A treatment on the basis of the Michaelis−Menten approach, originally developed for enzyme kinetics, was therefore applied and linearized by means of a Lineweaver−Burk plot (double reciprocal) to calculate various kinetic parameters such as the Michaelis−Menten constant ($K_M = 1.7(3)\times10^{-4}$ for all three complexes) and maximum initial rate (Vmax = 5.20 $(3)\times10^{-4}$ M min^{-1} for complex **1**, 7.2(3) $\times10^{-5}$ M.min^{-1} for complex **2** and $6.9(3)\times10^{-5}$ for complex **3**). The turnover number of the complex (k_{cat} = 177 h^{-1} for complex **1**, 432 h^{-1} for complex **2** and 426 h^{-1} for complex **3** per metal centre) is calculated by dividing the V_{max} value by the concentration of the complex.

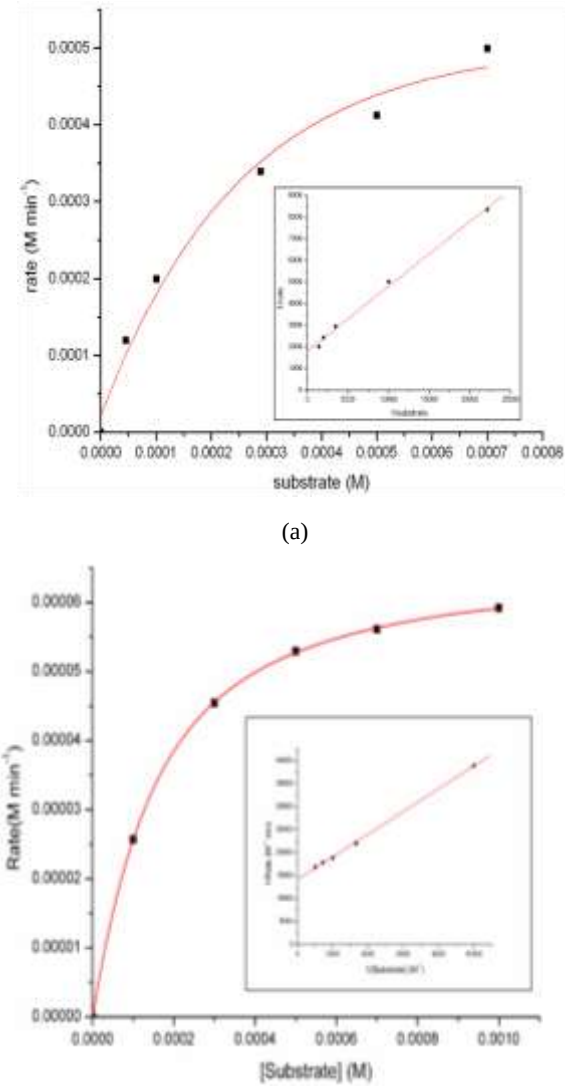

Fig. 9 Plot of initial rates vs substrate concentration for the oxidation reaction catalyzed by complex **1** (Fig. 9(a)) and complex **2** (Fig. 9(b)). Inset shows the Lineweaver−Burk plot.

The oxidation process of 3,5-DTBC to 3,5-DTBQ involves two electrons. A literature survey reveals that higher valent metal centers (e.g., Cu^{II}, Mn^{III} and Mn^{IV})[30,31] are usually involved in catechol oxidation, while reports on catecholase activities of manganese(II) complexes are relatively rare.[32] The manganese centers are in +2 and +3 oxidation states in complexes **2** and **3**. Therefore, it is reasonable to consider that in the catalytic cycle

performed by complexes **2** and **3** , Mn(III) undergoes reduction to Mn(II) with concomitant oxidation of 3,5-DTBC to 3,5-DTBQ in the presence of molecular oxygen. Turnover number of the complex **2** and **3** (432 h^{-1} and 426 h^{-1} per metal centre) is higher than those of Krebs et al. and Rajak et al.[33,34] and comparable to those reported by Vittal et al.[35] and Das et al.[29] On the other hand, catechol oxidation catalyzed by Mn(II) complexes has been proposed to occur through the formation of Mn(III) and Mn(IV) species[32b]. The turnover number of complex **1** (177 h^{-1}per metal centre) is comparatively lower than that reported by Das et al.[31a] and comparable to those reported by Krebs et al.[33]

Conclusions

A 2D coordination polymer of Mn^{II}, Mn(*o*-$(NO_2)C_6H_4COO)_2{\cdot}3H_2O$ has been prepared by reacting pyz with Mn(*o*-$(NO_2)C_6H_4COO)_2{\cdot}3H_2O$ in 1:1 molar ratio. The compound did not undergo aerial oxidation in acetonitrile solution unlike its benzoate or phenyl acetate analogues; instead it needed oxidizing agent, *n*-Bu_4NMnO_4, to produce hexanuclear Mn(II/III) complexes based on $[Mn^{III}{}_2Mn^{II}{}_4O_2]^{10+}$ units. The product was crystallized from two solvents (acetonitrile and acetone) and structural analysis of both showed that only one of the four solvent molecules of $[Mn^{III}{}_2Mn^{II}{}_4O_2]^{10+}$ units was partially replaced by the pyrazine molecule. The results are in sharp contrast to that of the phenyl acetate analogue where all four solvent molecules have been replace by pyrazine to form a diamondoid metal-organic framework. Variable-temperature (1.8-300 K) magnetic susceptibility measurements showed the presence of antiferromagnetic coupling through the *syn-anti* carboxylate bridge in compound **1**. The modelling of the magnetic results of **2** and **3** revealed that the magnetic coupling between the central Mn^{III} ions is strong and other exchange pathways are less relevant, a result that is usual for such complexes. All three complexes showed catecholase-like activity and the Michaelis–Menten approach to enzyme catalysis has been applied to rationalize the kinetic parameters. Considerably higher turnover numbers of **2** and **3** compared to **1** clearly indicate that the presence of higher valent manganese (Mn^{III}) enhances their catecholase-like activity.

Acknowledgements

We thank DST-FIST, India funded Single Crystal Diffractometer Facility at the Department of Chemistry, University of Calcutta, Kolkata, India. P.K. is thankful to DST-PURSE, India for funding.

Notes and references

[a]*Department of Chemistry, University College of Science, University of Calcutta, 92, A.P.C. Road, Kolkata-700 009, India; E-mail: ghosh_59@yahoo.com*

[b]*Department of Engineering Science, The University of Electro-Communications, Chofu, Tokyo 182-8585, Japan*

[c]*School of Chemistry, The University of Reading, P.O BOX 224, Whiteknights, Reading RG6 6AD, U.K.*

*†Electronic supplementary information (ESI) available: The electronic supplementary information file contains Figure S1-S2. Table ST1. CCDC 1049356-1049358 for **1-3**. For ESI and crystallographic data in CIF or other electronic format see DOI: 10.1039/*

1 (*a*) E. Cremades, J. Cano, E. Ruiz, G. Rajaraman, C. J. Milios and E. K. Brechin, *Inorg. Chem.*, 2009, **48**, 8012–8019; (*b*) N. Lima, A. Caneschi, D. Gatteschi, M. Kritikos and L. G. Westin, *Inorg. Chem.*, 2006, **45**, 2391–2393; (*c*) A. J. Tasiopoulos, W. Wernsdorfer, K. A. Abboud and G. Christou, *Angew. Chem., Int. Ed.*, 2004, **43**, 6338–6342; (*d*) C. C. Stoumpos, R. Inglis, O. Roubeau, H. Sartzi, A. A. Kitos, C. J. Milios, G. Aromi, A. J. Tasiopoulos, V. Nastopoulos, E. K. Brechin and S. P. Perlepes, *Inorg. Chem*., 2010, **49**, 4388–4390; (*e*) C. C. Stoumpos, R. Inglis, G. Karotsis, L. F. Jones, A. Collins, S. Parsons, C. J. Milios, G. S. Papaefstathiou and E. K. Brechin, *Cryst. Growth Des.*, 2009, **9**, 24–27; (*f*) S. G. Baca, I. L. Malaestean, T. D. Keene, H. Adams, M. D. Ward, J. Hauser, A. Neels and S. Decurtins, *Inorg. Chem.*, 2006, **47**, 11108–11119; (*g*) P. Kar, R. Biswas, M. G. B. Drew, Y. Ida, T. Ishida and A. Ghosh, *Dalton Trans*., 2011, **40**, 3295-3304; (*h*) S. Naiya, S. Biswas, M. G. B. Drew, C. J. Gómez-García and A. Ghosh, *Inorg. Chem*., 2012, **51**, 5332–5341; (*i*) P. Kar, P. M. Guha, M. G. B. Drew, T. Ishida and A. Ghosh, *Eur. J. Inorg. Chem.*, 2011, 2075–2085; (j) P. Kar, R. Biswas, Y. Ida, T. Ishida, and A. Ghosh, *Cryst. Growth Des.*, 2011, **11**, 5305–5315.

2 (*a*) K. N. Ferreira, T. M. Iverson, K. Maghlaoui, J. Barber and S. Iwata, *Science*., 2004, **303**, 1831−1838; (*b*) A. W. Rutherford and A. Boussac, *Science*, 2004, **303**, 1782−1784; (*c*) S. Mukhopadhyay, S. K. Mandal, S. Bhaduri and W. H. Armstrong, *Chem. Rev.*, 2004, **104**, 3981−4026; (*d*) F. Rappaport and B. A. Diner, *Coord. Chem. Rev.*, 2008, **252**, 259−272; (*e*) M. Carboni and J.-M. Latour, *Coord. Chem. Rev.*, 2011, **255**, 186−202.

3 (*a*) D. Lieb, A. Zahl, T. E. Shubina and I. Ivanovic-Burmazovic, *J. Am. Chem. Soc.*, 2010, **132**, 7282−7284; (*b*) I. Kani, C. Darak, O. Şahin and O. Büyükgüngör, *Polyhedron*, 2008, **27**, 1238−1247; (*c*) G. Maayan and G. Christou, *Inorg. Chem*., 2011, **50**, 7015−7021; (*d*) P. Mukherjee, P. Kar, S. Ianelli and A. Ghosh, *Inorg. Chim. Acta*, 2011, **365**, 318−324.

4 (*a*) D. Shen, C. Miao, S. Wang, C. Xia and W. Sun, *Eur. J. Inorg. Chem.*, 2014, 5777–5782; (*b*) S. Kal, L. Ayensu-Mensah and P. H. Dinolfo, *Inorg. Chim. Acta*, 2014, **423**, 201–206; (*c*) T. Katsuki, *Coord. Chem. Rev.*, 1995, **140**,189-214.

5 (*a*) P. Mahata, D. Sarma and S. Natarajan, *J. Chem. Sci.*, 2010, **122**, 19–35; (*b*) X.-Y. Wang, H.-Y. Wei, Z.-M. Wang, Z.-D. Chen and S. Gao, *Inorg. Chem.* 2005, **44**, 572−583; (*c*) G. Beobide, O. Castillo, A. Luque, U. Garcia-Couceiro, J. P. Garcia-Teran and P. Roman, *Dalton Trans.*, 2007, 2669–2680; (*d*) J. Cano, T. Cauchy, E. Ruiz, C. J. Milios, C. C. Stoumpos, T. C. Stamatatos, S. P. Perlepes, G. Christou and E. K. Brechin, *Dalton Trans.*, 2008, 234–240.

6 (*a*) C. Lampropoulos, G. Redler, S. Data, K. A. Abboud, S. Hill and G. Christou, *Inorg. Chem.*, 2010, **49**, 1325−1336; (*b*) H.

Miyasaka, A. Saitoh and S. Abe, *Coord. Chem. Rev.*, 2007, **251**, 2622−2664; (*c*) J. S. Costa, L. A. Barrios, G. A. Craig, S. J. Teat, F. Luis, O. Roubeau, M. Evangelisti, A. Camón and G. Aromí, *Chem. Commun.* 2012, **48**, 1413−1415; (*d*) K. C. Mondal, Y. Song and P. S. Mukherjee, *Inorg. Chem.*, 2007, **46**, 9736−9742; (*e*) K. C. Mondal, M. G. B. Drew and P. S. Mukherjee, *Inorg. Chem*., 2007, **46**, 5625−5629.

7 (*a*) T. C. Stamatatos, K. A. Abboud and G. Christou, *J. Mol. Struct.* 2008, **890**, 263–271; (*b*) H. Oshio, N. Hoshino, T. Ito, M. Nakano, F. Renz and P. Gutlich, *Angew. Chem., Int. Ed*., 2003, **42**, 223-225.

8 (*a*) A. R. Schake, J. B. Vincent, Q. Li, P. D. W. Boyd, K. Folting, J. C. Huffman, D. N. Hendrickson and G. Christou, *Inorg. Chem.*, 1989, **28**, 1915-1923; (*b*) E. E. Moushi, A. J. Tasiopoulos and M. J. Manos, *Bioinorg Chem Appl.*, 2010, 367128-367135; (*c*) D. M. Low, E. K. Brechin, M. Helliwell, T. Mallah, E. Rivière and E. J. L. McInnes, *Chem. Commun*., 2003, 2330–2331; (*d*) J. Kim and H. Cho, *Inorg. Chem. Commun*., 2004, **7**, 122–124.

9 P. Gerbier, D. Ruiz-Molina, J. Gomez, K. Wurst and J. Veciana, *Polyhedron*, 2003, **22**, 1951-1955.

10 L. A. Kushch, G. V. Shilov, R. B. Morgunov and E. B. Yagubskii, *Mendeleev Commun*., 2009, **19**, 170–171.

11 P. Kar, R. Haldar, C. J. Gómez-García and A. Ghosh, *Inorg. Chem*., 2012, **51**, 4265−4273.

12 P. Seth and A. Ghosh, *RSC Adv*., 2013, **3**, 3717-3725.

13 (*a*) J. B. Vincent , K. Folting , J. C. Huffman and G. Christou, *Inorg. Chem*., 1986, **25**, 996–999.

14 W. Ferenc, *Gazz. Chim. Ital.*, 1995, **125**, 6–23.

15 SAINT, version 6.02; SADABS, version 2.03; Bruker AXS, Inc.:Madison, WI, 2002.

16 G. M. Sheldrick, SHELXS 97, Program for Structure Solution; University of Gottingen: Germany, 1997.

17 G. M. Sheldrick, SHELXL 97, Program for Crystal Structure Refinement; University of Gottingen: Germany, 1997.

18 A. L. Spek, PLATON. *Molecular Geometry Program. J. Appl. Crystallogr*., 2003, **36**, 7–13.

19 L. J. Farrugia, *J. Appl. Crystallogr.*, 1997, **30**, 565.

20 L. J. Farrugia, *J. Appl. Crystallogr*., 1999, **32**, 837–838.

21 T. C. Stamatatos, D. Foguet-Albiol, S. P. Perlepes, C. P. Raptopoulou, A. Terzis, C. S. Patrickios, G. Christou and A. J. Tasiopoulos, *Polyhedron*, 2006, **25**, 1737−1746.

22 M. E. Fisher, *Am. J. Phys.*, 1964, **32**, 343-346.

23 M. E. Lines, *J. Phys. Chem. Solids*, 1970, **31**, 101-116.

24 (*a*) D. K. Towle, K. Hoffmann, W. E. Hatfield, P. Singh and P. Chaudhuri, *Inorg. Chem.*, 1988, **27**, 394–399; (*b*) E. Colacio, J.-M. Dominguez-Vera, J.-P. Costes, R. Kivekas, J.-P. Laurent, J. Ruiz and M. Sundberg, *Inorg. Chem*., 1992, **31**, 774–778.

25 (*a*) R. L. Carlin, K. Kopinga, O. Kahn and M. Verdaguer, *Inorg. Chem.* 1986, 25, 1786–1786; (*b*) F. Lloret, Julve, M. Julve, R. Ruiz, Y. Journeaux, K. Nakatani, O. Kahn and J. Sletten, *Inorg. Chem*., 1993, **32**, 27–31.

26 MAGPACK: Magnetic Properties Analysis Package for Spin Clusters, J. J. Borrás-Almenar, J. M. Clemente-Juan, E. Coronado and B. Tsukerblat, Univ. de Valencia, Spain, 2000.

27 (*a*) C.-B. Ma, M.-Q. Hu, H. Chen, C.-N. Chen and Q.-T. Liu, *Eur. J. Inorg. Chem*., 2008, 5274−5280; (*b*) E. Fursova, V. Ovcharenko, K. Nosova, G. Romanenko and V. Ikorskii, *Polyhedron*, 2005, **24**, 2084−2093; (*c*) V. Ovcharenko, E. Fursova, G. Romanenko and V. Ikorskii, *Inorg. Chem.*, 2004, **43**, 3332−3334; (*d*) J. Kim and H. Cho, *Inorg. Chem. Commun*. 2004, 7, 122−124; (*e*) A. R. E. Baikie, A. J. Howes, M. B. Hursthouse, A. B. Quick and P. Thornton, *J. Chem. Soc., Chem. Commun.*, 1986, 1587−1587; (*f*) L. A. Kushch, G. V. Shilov, R. B. Morgunov and E. B. Yagubskii, *Mendeleev Commun.*, 2009, **19**, 170−171; (*g*) E. Ruiz and S. Alvarez, *Chem. Commun*., 1998, 2767−2768.

28 J. Mukherjee and R. Mukherjee, *Inorg. Chim. Acta*, 2002, **337**, 429−438.

29 K. S. Banu, T. Chattopadhyay, A. Banerjee, M. Mukherjee, S. Bhattacharya, G. K. Patra, E. Zangrando and D. Das, *Dalton Trans.*, 2009, 8755−8764.

30 (*a*) I. A. Koval, P. Gamez, C. Belle, K. Selmeczi and J. Reedijk, *Chem. Soc. Rev.*, 2006, **35**, 814−840; (*b*) V. K. Bhardwaj, N. Aliaga-Alcalde, M. Corbella and G. Hundal, *Inorg. Chim. Acta*, 2010, **363**, 97−106.

31 (*a*) S. Mukherjee, T. Weyhermuller, E. Bothe, K. Wieghardt and P. Chaudhuri, *Dalton Trans.*, 2004, 3842−3853; (*b*) A. Majumder, S. Goswami, S. R. Batten, M. S. E. Fallah, J. Ribas and S. Mitra, *Inorg. Chim. Acta*, 2006, **359**, 2375−2382; (*c*) S. E. Jones, D.-H. Chin and D. T. Sawyer, *Inorg. Chem.*, 1981, **20**, 4257−4262.

32 (*a*) A. Guha, K. S. Banu, A. Banerjee, T. Ghosh, S. Bhattacharya, E. Zangrando and D. Das, *J. Mol. Catal. A: Chem.*, 2011, **338**, 51−57; (*b*) J. Kaizer, G. Barath, R. Csonka, G. Speier, L. Korecz, A. Rockenbauer and L. J. Parkanyi, *Inorg. Biochem*., 2008, **102**, 773−780; (*c*) M. Kloskowski and B. Krebs, *Z. Anorg. Allg. Chem.*, 2006, **632**, 771−778.

33 M. U. Triller, D. Pursche, W.-Y. Hsieh, V. L. Pecoraro, A. Rompel and B. Krebs, *Inorg. Chem.*, 2003, **42**, 6274−6283.

34 (*a*) A. Banerjee, S. Sarkar, D. Chopra, E. Colacio and K. K. Rajak, *Inorg. Chem.*, 2008, **47**, 4023−4031; (*b*) A. Banerjee, R. Singh, E. Colacio and K. K. Rajak, *Eur. J. Inorg. Chem*., 2009, 277−284.

35 B. Sreenivasulu, M. Vetrichelvan, F. Zhao, S. Gao and J. J. Vittal, *Eur. J. Inorg. Chem*., 2005, 4635−4645.